

Structural and optical properties of silica capped ZnS:Mn quantum dots

Sunil Kumar¹ · H. C. Jeon¹ · T. W. Kang¹ · Rajan Singh² · J. K. Sharma² · Ravi Kant Choubey³

Received: 9 December 2014 / Accepted: 10 March 2015 / Published online: 15 March 2015
© Springer Science+Business Media New York 2015

Abstract In the present work, the structural and optical properties of Silica capped ZnS:Mn quantum dots (QDs) has been reported. Chemical precipitation technique was used to form the core–shell nanostructures. The results indicate that the Silica capped ZnS:Mn QDs has cubic Zinc Blende structure and its grain size is about 2 nm as demonstrated by X-ray diffraction (XRD). Transmission electron microscopy images showed that the presence of Silica capping on ZnS:Mn QDs can prevent their agglomeration by cluster formation and their particle size (2–3 nm) well matches with XRD results. The selected area diffraction pattern shows a set of sharp rings corresponding to the (111), (220) and (311) lattice planes of the cubic phase of ZnS which proves the polycrystalline behaviour. Band gap studies were done by UV–visible spectroscopy and presence of Silica have been confirmed by EDAX and FTIR analysis. Photoluminescence studies shows emission wavelength as well as intensity to be tunable with Silica capping. As Silica capped ZnS:Mn QDs can control various parameters of ZnS:Mn, they are suitable material for specific kind of tunable optoelectronic devices.

1 Introduction

Semiconductor Quantum dots (QDs) have been extensively investigated during the last two decades due to their unique size-dependent properties [1–3] and promising technological application potential [4–9]. Due to the strong confinement effects of the QDs, the properties of these nanocrystallites vary significantly with their size. The optical properties of these materials can be easily tuned to suit potential applications in the area of optoelectronic devices [10].

Among the semiconductor QDs, Zinc Sulfide (ZnS) have been widely used in optoelectronics devices due to its wide band gap value. Doping with transition metal ions such as Mn²⁺ ions not only enhance the optical transition efficiency and increase the number of the luminescent centers but also inspire them to exhibit interesting magneto-optical properties [11–13]. Upon excitation, the Mn²⁺ doped ZnS nanostructures produce characteristic bright yellow–orange emission 585 nm due to the 4T₁ → 6A₁ transition of Mn²⁺ [14]. Mn²⁺ doped ZnS nanoparticles and thin films have been widely studied by several groups [15–17]. But their practical applications remain very limited due to the heavy dependence of the optical properties on the size of the QDs and nature of their capping [18]. Enhanced luminescence and stability have been observed in ZnS:Mn/ZnO nanocrystals [19]. Since, ZnO has a very high binding energy as well as good chemical and thermal stability, so the inverted core–shell combination of ZnS:Mn/ZnO seems to be very attractive. According to the previous literature, Daixun et al. [20] studied the influence of ZnO shell thickness on the luminescence properties of Mn²⁺ doped ZnS nanoparticles. A strong increase followed by a gradual decline was observed in the room temperature photoluminescence (PL) spectra with the thickening of the ZnO shell. Recently, Ashkarran et al. [21] has prepared Mn

✉ Ravi Kant Choubey
ravikantchoubey@gmail.com

¹ Quantum Functional Semiconductor Research Center, Dongguk University, Seoul 100715, South Korea

² Department of Physics, Maharishi Markandeshwar University, Mullana, Ambala 133207, India

³ Department of Applied Physics, Defence Institute of Advanced Technology, Girinagar, Pune 411025, India

doped ZnS nanoparticles using wet chemical method at room temperature and observed that a remarkable difference in photocatalytic performance of Mn doped ZnS. A comprehensive parametric optimisation for the synthesis of Mn doped ZnS nanoparticles have been well studied by Sen et al. [22]. Recently, we have observed the photo-physical studies of pyridine capped ZnO Nanostructures and the effect of zinc oxide concentration in fluorescent ZnS:Mn/ZnO core-shell nanostructures. It was found that emission wavelength is red shifted with the addition of ZnO layer on ZnS:Mn [23, 24]. It is clear from the survey that lot of work has been done on ZnS:Mn nanostructures and some work on ZnS core-shell nanostructures but almost very less work has been done using Silica as a coating agent [25, 26]. In this report, we employed Silica capping on ZnS:Mn QDs. The main advantage of this capping is that it saturates the surface dangling bonds on the surface which reduces the generation of the surface-passivated “dead layers”. Moreover, Silica is an ideal inorganic capping material for ZnS QDs since its refractive index is significantly lower than the refractive index of ZnS [27]. Furthermore, Silica acts as a good binder, has a wide band gap (9.1 eV) and has an amorphous structure [28].

In the present paper, ZnS:Mn and Silica capped ZnS:Mn QDs were synthesised by chemical precipitation method and the synthesis reaction was carried out in the aqueous medium. The evolution of the structural, optical and morphological properties of the Silica capped ZnS:Mn QDs have been studied by Energy Dispersive X-ray analysis (EDX), X-Ray diffraction (XRD), UV-visible, Fourier transformation infrared (FTIR), energy resolved PL spectroscopy and Transmission electron microscopy (TEM). Very interesting results were obtained in comparison to the earlier reports from the same group. However the results seem to be promising in terms of the tunability which is highly desirable in several optoelectronic applications such as electro-optic modulators, infrared windows, electroluminescent display etc.

2 Experimental details

2.1 Synthesis of ZnS:Mn QDS

The ZnS:Mn quantum dots were synthesized by chemical precipitation method, which has been reported very recently [23]. The synthesis reaction was carried out in the aqueous medium. Homogeneous solutions of 0.5 M Zinc Acetate ($\text{Zn}(\text{CH}_3\text{COO})_2 \cdot \text{H}_2\text{O}$), 0.01 M of Manganese Acetate ($\text{Mn}(\text{CH}_3\text{COO})_2$) and 0.5 M Sodium Sulphide (Na_2S) were prepared by dissolving 5.487 g of Zinc Acetate, 0.1225 g of Manganese Acetate and 1.951 g of Sodium Sulphide in 50 ml of water separately and stirring for 30 min. 0.5 ml solution was taken away from Zinc Acetate

solution and 29.75 ml of Manganese Acetate solution was added instead into the Zinc Acetate solution. The optimum value of Mn used in this work is 1 % to get the maximum PL intensity as already proved from the earlier work by the same authors [23]. The resultant solution was stirred with magnetic stirrer for 30 min. Then 0.5 M Sodium Sulphide solution was added drop wise to the 0.5 M solution of Zinc Acetate and Manganese Acetate combined solution. Soon after the addition of Sodium Sulphide solution, precipitation phenomenon occurred and the concentration of precipitates increased with the increase in Sodium Sulphide solution. The stirring was allowed for 1 h at room temperature using a magnetic stirrer. Then the particles were centrifuged at 1000 rpm for 5 min. The precipitated particles were filtered using Whatman 40 filter paper. The particles were washed several times using de-ionized water to remove the last traces of adhered impurities. The washed particles were dried at 60 °C for 24 h in vacuum oven and crushed the sample into powder to get the ZnS:Mn QDs.

2.2 Synthesis of tetraethyl orthosilicate capped ZnS:Mn QDS

Homogeneous ZnS:Mn powder was taken by three different amounts as 0.8, 1.6 and 3.2 g. It was added to 50 ml Ethanol and stirred with magnetic stirrer for 30 min. Then Tetraethyl Orthosilicate (5 ml) was added drop wise to the solution. Then stirring was allowed for 15 min at room temperature using a magnetic stirrer and the particles were centrifuged at 1000 rpm for 5 min. The precipitated particles were filtered using Whatman 40 filter paper. The particles were washed several times using de-ionized water to remove the last traces of adhered impurities. The washed particles were dried at 60 °C for 24 h in vacuum oven. Thus we obtained Silica coated ZnS:Mn Quantum Dots.

3 Characterization

X-ray diffraction patterns of ZnS:Mn and Silica capped ZnS:Mn quantum dots (in various capping concentrations) were examined by using Bruker AXS, D8 Advance X-ray diffractometer with a copper target operated at 40 kV and 30 mA. The data collection steps were in intervals of 0.05°. The low and high resolution bright field transmission microscopic images were taken on Hitachi (H-7500) transmission microscope operating at an acceleration voltage of 200 kV. The EDAX analysis was also done to confirm the presence of Si in the Silica capped ZnS:Mn quantum dots. Optical absorbance of the ZnS:Mn and Silica capped ZnS:Mn quantum dots were recorded with a double beam UV-visible spectrophotometer (Model: Hitachi—330) in the range of 200–800 nm. Fourier transform infrared (FTIR)

Fig. 1 X-ray diffraction spectrum of *a* 3.2 g ZnS:Mn *b* 1.6 g ZnS:Mn *c* 0.8 g ZnS:Mn *d* ZnS:Mn samples

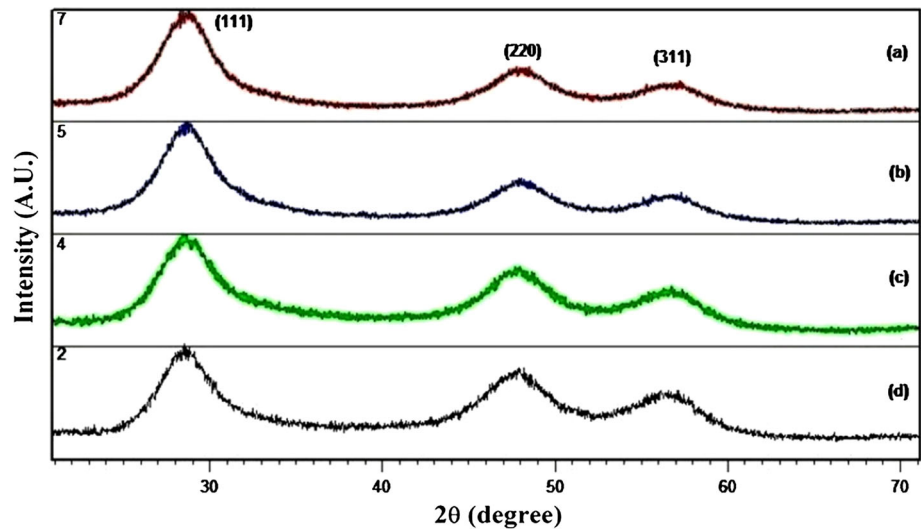


Table 1 Variation in crystallite size and band gap of uncapped and silica capped ZnS:Mn QDs

| S. no. | Samples | Crystallite size (nm) from (111) peak | Band gap (eV) |
|--------|--------------|---------------------------------------|---------------|
| 1 | ZnS:Mn | 1.962 | 3.77 |
| 2 | 0.8 g ZnS:Mn | 2.197 | 3.79 |
| 3. | 1.6 g ZnS:Mn | 2.116 | 3.84 |
| 4 | 3.2 g ZnS:Mn | 2.238 | 3.78 |

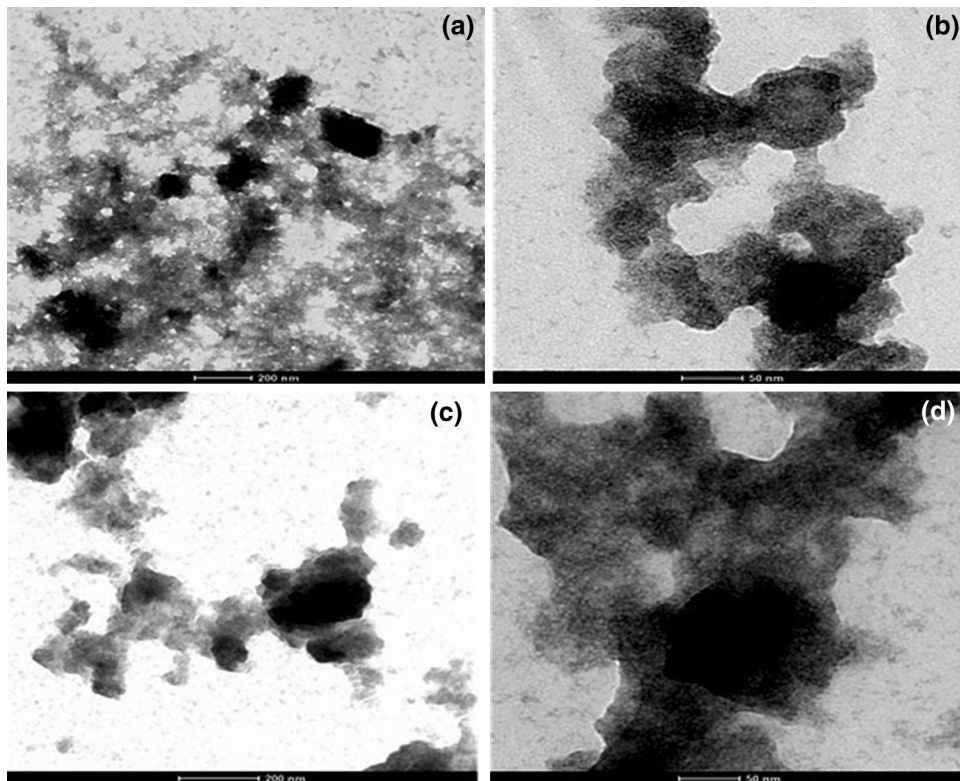


Fig. 2 TEM image of *a* ZnS:Mn *b* 0.8 g ZnS:Mn *c* 1.6 g ZnS:Mn *d* 3.2 g ZnS:Mn QDs

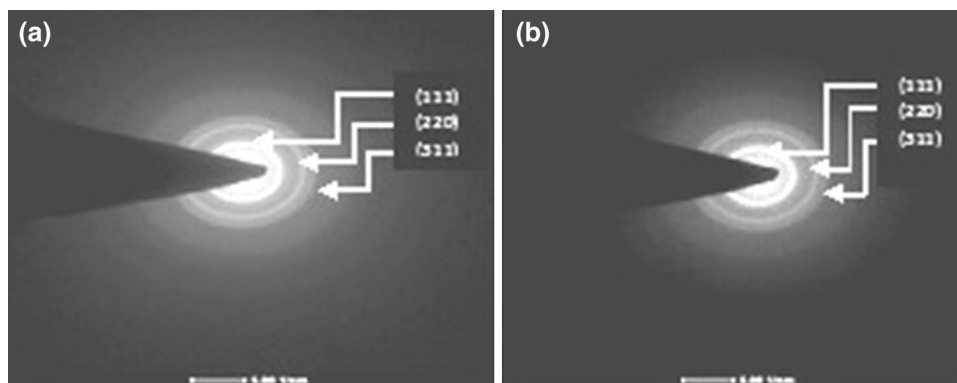


Fig. 3 SAED pattern of **a** ZnS:Mn **b** 1.6 g ZnS:Mn

spectra were recorded in range of $4000\text{--}400\text{ cm}^{-1}$ with Perkin Spectrum RXI (40). Energy resolved PL studies were conducted by Perkin Elmer LS (50B) fluorescence spectrometer and the Xenon lamp was used as the excitation source.

4 Results and discussions

4.1 Structural studies

Figure 1 shows XRD pattern of silica capped (3.2, 1.6 and 0.8 g) ZnS:Mn and ZnS:Mn QDs. The spectra were obtained by scanning 2θ in the range $10^\circ\text{--}60^\circ$, with a grazing angle equal to 0.02° . The identification and assignments of the observed diffraction patterns are made using the JCPDS data and reported literature [29, 30]. As it is well known, bulk ZnS can exist in two crystalline modifications: the hexagonal (wurtzite) phase and the cubic (zinc blende) phase. The most stable form of ZnS is the cubic structure and in the bulk form it transforms to wurtzite structure at 1020°C . The results of X-ray analysis agreed well with the earlier reported results [29, 30].

In Fig. 1, the diffraction patterns showed three broad diffraction peaks at 28.5° , 47.6° and 56.4° are corresponded to the (111), (220), and (311) planes in the β -ZnS cubic structure. Broadening of XRD peaks shows the formation of nanocrystals of ZnS:Mn. It is to be noted that, doping of Mn^{2+} ions and capping of silica into ZnS did not create a phase change. The average crystallite size D calculated from the XRD patterns using the Scherer formula was found to be about 2 nm (Table 1). Single phase formation of all ZnS:Mn QDs may be interpreted as due to the nanocrystalline size of the present samples.

4.2 Surface morphology studies

To get the optimum information regarding the morphology of the samples, a detailed investigations on the samples

have been done by low and high resolution bright field transmission electron microscope (TEM).

The specimen preparation has been done by finely dispersing the nanoparticles in spectroscopic grade ethanol and then putting a drop of the dispersed solution on the carbon coated copper grid. Figure 2a–d shows the TEM images of uncapped and silica capped ZnS:Mn QDs. It can be noticed from the TEM micrographs, that uncapped ZnS:Mn QDs are fully agglomerated but Silica capped ZnS:Mn QDs looks like cluster of particles. Hence presence of silica capping on ZnS:Mn nanoparticles can prevent the agglomeration of all QDs in the form of bunch of clusters. Also, it is observed from TEM pictures that diameters of most of the particles lie in the range of 2–3 nm, which is also in agreement with the XRD results.

Figure 3 shows selected area diffraction (SAED) pattern for uncapped and silica capped ZnS:Mn QDs. The SAED pattern shows a set of sharp rings corresponding to

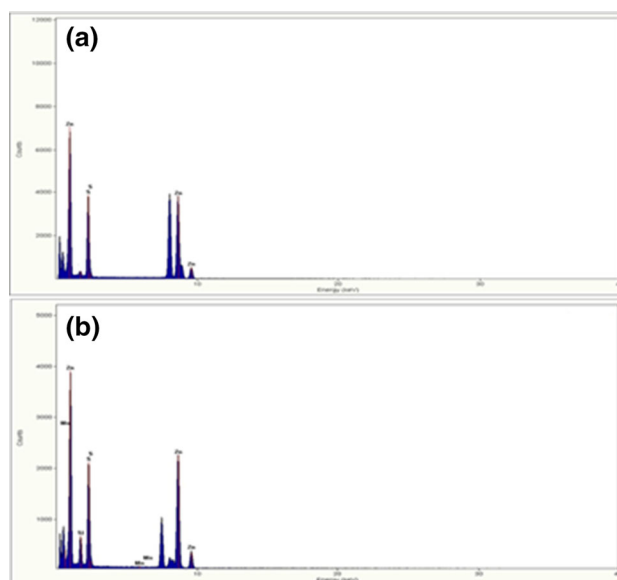


Fig. 4 EDAX of **a** ZnS:Mn **b** 1.6 g ZnS:Mn QDs

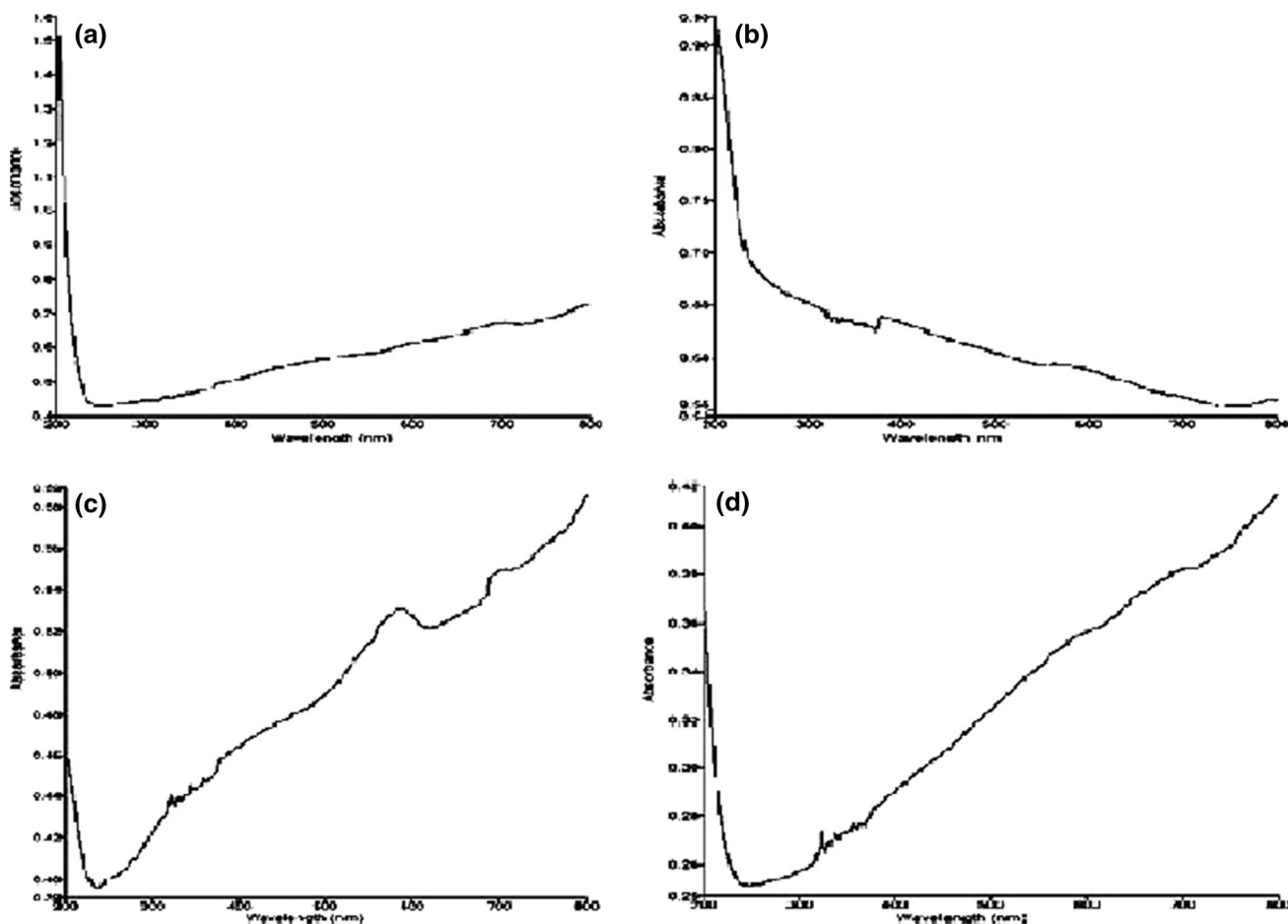


Fig. 5 UV-visible absorption spectra of **a** ZnS:Mn **b** 0.8 g ZnS:Mn **c** 1.6 g ZnS:Mn **d** 3.2 g ZnS:Mn QDs

diffraction from different planes of the nanocrystallites instead of spots due to the random orientation of the crystallites. It is evidently observed three rings corresponding to the (111), (220) and (311) lattice planes of the cubic phase of ZnS, which is also in good agreement with the above XRD patterns. The EDAX of the uncapped and silica capped ZnS:Mn QDs have been presented in Fig. 4a–b. In Fig. 4a, The trace of Zn, S, Mn is observed while in Fig. 4b trace of Si also present along with the above mentioned elements, which again confirms the presence of Si capping in ZnS:Mn QDs.

4.3 Optical studies

The variations of optical absorbance as a function of wavelength for ZnS:Mn and silica capped ZnS:Mn QDs are shown in Fig. 5a–d. The absorption peaks for uncapped, 0.8 g ZnS:Mn, 1.6 g ZnS:Mn, and 3.2 g ZnS:Mn silica capped QDs are found at 321, 323, 318, 319 nm respectively.

For calculating the direct band gap value $(\alpha hv)^2$ versus hv is plotted by extrapolating the straight portion of the graph (Fig. 6) on hv axis at $\alpha = 0$, the values of calculated

optical band gaps are given in Table 1. It can be noticed that 1.6 g ZnS:Mn silica capped QDs have maximum band gap i.e. 3.84 eV, which shows better confinement effect compared to other capped and uncapped samples while strong quantum confinement effect is observed in all the samples in comparison to the bulk ZnS which has a band gap of 3.68 eV.

Particle size for different samples has also been calculated by using Brus equation [31]. A computer code, for Brus equation was used for the calculation of particle size of uncapped and silica capped ZnS:Mn QDs. In these calculations, band gap of QDs (E_{np}) was used as calculated from the $(\alpha hv)^2$ versus hv graph. The Brus equation is:

$$E_{np} = E_g + \frac{h^2}{8r^2} \left[\frac{1}{m_e^*} + \frac{1}{m_h^*} \right] - \frac{1.8e^2}{\epsilon r} \tag{1}$$

where E_g is band gap of bulk ZnS, which is 3.68 eV, r is the radius of the nanoparticle in nanometers, m_e^* is the effective mass of the electron, m_e is the mass of an electron (for ZnS, $m_e^* = 0.25 m_e$), m_h^* is the effective mass of the hole, m_h is the mass of a hole (for ZnS $m_h^* = 0.60 m_e$), e is the charge on the electron, ϵ is the dielectric constant of

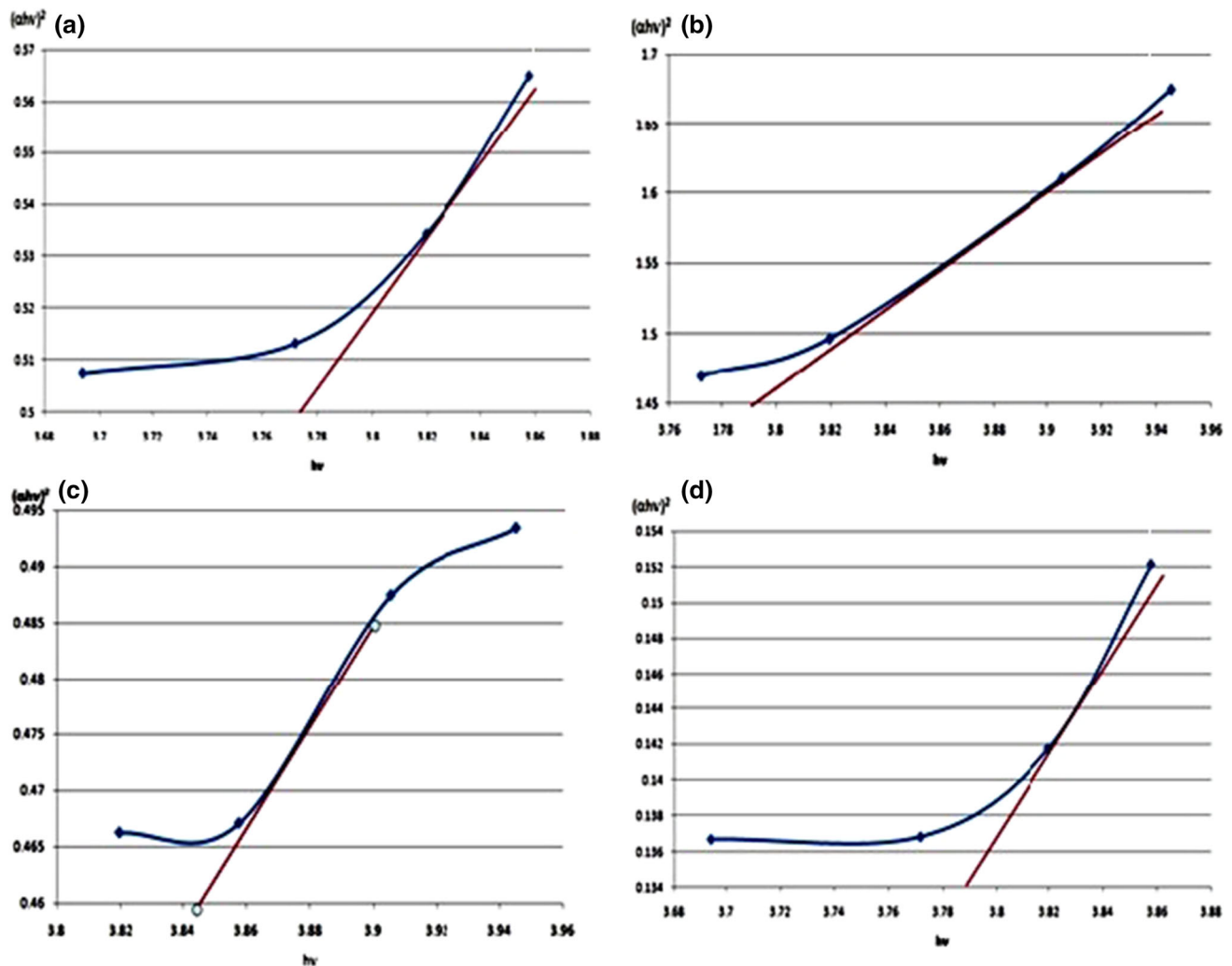


Fig. 6 Optical band gap for **a** ZnS:Mn **b** 0.8 g ZnS:Mn **c** 1.6 g ZnS:Mn **d** 3.2 g ZnS:Mn QDs

material (for ZnS, $\epsilon = 8.3$) and ϵ_0 is the vacuum permittivity constant.

The average particle sizes computed according to the Eq. 1 for uncapped Mn:ZnS, 0.8 g ZnS:Mn, 1.6 g ZnS:Mn and 3.2 g ZnS:Mn quantum dots are 3.05, 2.96, 2.77 and 2.84 nm respectively. As the Bohr exciton radius in case of ZnS quantum dots is 5 nm and we are getting average particle size <5 nm using Brus equation. Thus, from the theoretical calculations, quantum confinement effect in case of Silica capped ZnS:Mn quantum dots is once again proved in similarity to XRD and TEM results.

4.4 FTIR studies

FTIR spectra is a powerful tool to provide information regarding the interaction of ZnS:Mn with the capping agent i.e. Silica. A small amount of quantum dots were

milled with KBr and then pressed into a disc for FTIR analysis [Perkin Spectrum RXI (40)] in order to investigate the surface properties of synthesized samples. Figure 7a–d shows FTIR spectra for ZnS:Mn and silica capped ZnS:Mn QDs in the range $4000\text{--}400\text{ cm}^{-1}$. It has been reported by several authors that around 3400 cm^{-1} a strong absorption band exist due to the hydrogen stretching frequency (OH^- ions stretching) [32, 33]. Air always contains a certain degree of humidity from which OH^- ions are incorporated into the lattice. Two principal absorption peaks are observed between 1650 and 1400 cm^{-1} corresponding to the asymmetric and symmetric stretching of the carboxyl group (C–O). The peak at 1106 cm^{-1} indicating that the doped Mn affected the structure of portion of the ZnS particles. The deformation bands of C–O can also be observed around 1015 cm^{-1} [34]. The bands around 1110 and 1186 cm^{-1} are due to

Fig. 7 FTIR spectra of ZnS:Mn and silica capped ZnS:Mn QDs

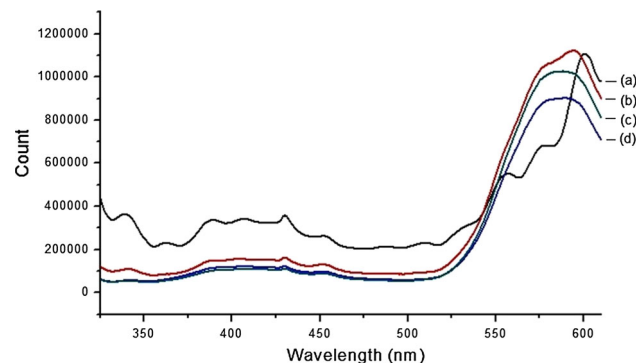
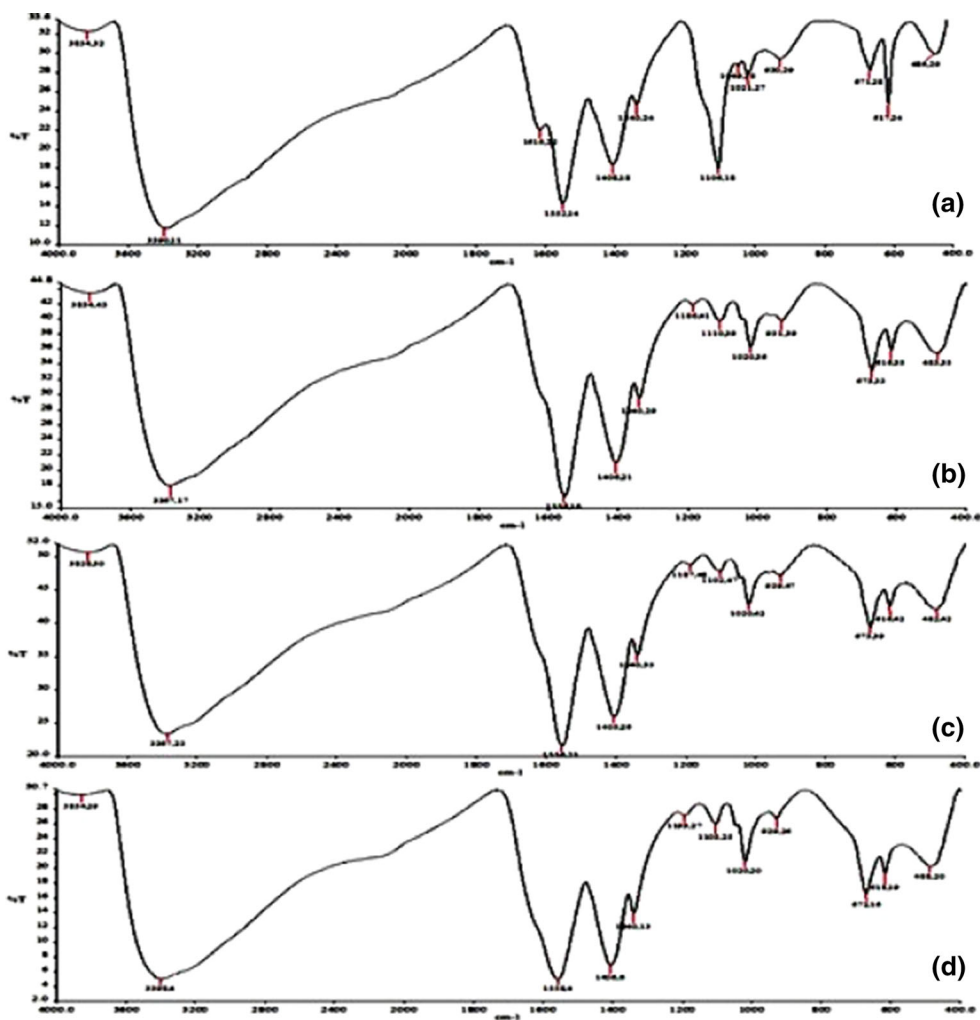


Fig. 8 Photoluminescence emission spectra of *a* ZnS:Mn *b* 0.8 g ZnS:Mn *c* 1.6 g ZnS:Mn *d* 3.2 g ZnS:Mn

Silica capping. The peak 486 cm^{-1} is assigned to the metal–oxygen bonds [35] while the peak positioned at 617 cm^{-1} originate from ZnS bond, possibly due to Zn–S stretching [36].

4.5 Photoluminescence studies

Energy resolved PL studies have been conducted to observe the possibility of tunability in the emission wavelength or emission intensity. Figure 8 shows the emission spectra, recorded at fixed excitation wavelengths which were taken from the absorption peaks of the UV–visible spectra. Subsequent transfer of electron and hole into the electronic level of the Mn ion leads to the characteristic emission of Mn^{2+} in ZnS. The two broad peaks at 542 and 570 nm in ZnS:Mn sample is seen where as these two peaks converts to a broad peak at 591 nm due to Silica capping in capped samples. So the Si capping effect can be observed in the three samples 0.8 g ZnS:Mn, 1.6 g ZnS:Mn and 3.2 g ZnS:Mn quantum dots. The emission data for the uncapped ZnS Quantum Dots and silica capped ZnS:Mn quantum dots are shown in above figure. The emission peak at 542 and 570 nm for uncapped QDs is blue shifted with respected to silica capped ZnS:Mn QDs. From the emission spectra, it is clear that emission intensity is

tuneable with silica capping which is very good for bio-labelling point of view and other applications.

5 Conclusion

In conclusion, ZnS:Mn QDs were prepared using Tetraethyl Orthosilicate as a capping agent by chemical precipitation method. The morphological and optical properties of ZnS:Mn QDs have been studied using XRD, TEM, UV–visible, FTIR and PL technique. XRD studies suggested a single phase formation. Also, doping of Mn²⁺ ions and capping of silica into ZnS did not create a phase change. The average crystallite size calculated by Debye–Scherrer formula was found to be 2–3 nm, which was again confirmed by TEM and Brus equations. The band gap was calculated using UV–visible spectra and observed strong quantum confinement effect in all the ZnS:Mn QDs samples in comparison to the bulk ZnS. PL studies demonstrates that emission wavelength as well emission intensity is tunable with silica capping which shows the utility of these samples in tuneable optoelectronic devices.

Acknowledgments This research was supported by Leading Foreign Research Institute Recruitment Program through the National Research of Korea (NRF) funded by the Ministry of Education, Science and Technology (MEST) (No.2014-039452). One of the author R. K. Choubey is thankful to Department of Science and Technology, Science and Engineering Research Board, New Delhi for the financial support (Grant No. SR/FTP/PS-038/2012) and Defence Institute of Advanced Technology, Girinagar, Pune for the financial support (Grant No. DAIT/F/REG(G)/BS/Proj/2014/2). One of the author is also thankful to the Department of Science (DST), New Delhi, India for supporting the part of this research work (vide Project No. SR/FTP/PS-69/2008), dated 15/1/2010.

References

1. X. Peng, L. Manna, W. Yang, J. Wickham, E. Scher, A. Kadavanch, A.P. Alivisatos, *Nature* **404**, 59 (2000)
2. S. Kim, B. Fisher, H. Eisler, M. Bawendi, *J. Am. Chem. Soc.* **125**, 11466 (2003)
3. L. Manna, D.J. Milliron, A. Meisel, E.C. Scher, A.P. Alivisatos, *Nat. Mater.* **2**, 382 (2003)
4. B. Sang, M. Konagai, *Jpn. J. Appl. Phys.* **35**, 602 (1996)
5. L. Bahadur, N.T. Rao, *J. Photochem. Photobiol. A: Chem.* **91**, 233 (1995)
6. Z. Hu, S. Chen, S. Peng, *J. Colloid Interface Sci.* **182**, 457 (1996)
7. D.M. Bagnall, Y.F. Chen, Z. Zhu, T. Yao, S. Koyama, M.Y. Shen, T. Goto, *Appl. Phys. Lett.* **70**, 2230 (1997)
8. M.H. Huang, S. Mao, H. Feick, H.Q. Yan, Y. Wu, H. Kind, E. Weber, R. Russo, P.D. Yang, *Science* **292**, 1897 (2001)
9. H. Kind, H.Q. Yan, B. Messer, M. Law, P.D. Yang, *Adv. Mater.* **14**, 158 (2001)
10. J. Ouyang, M. Vincent, D. Kingston, P. Descours, T. Boivineau, M.B. Zaman, X. Wu, K. Yu, *J. Phys. Chem. C* **113**, 5193 (2009)
11. V. Wood, J.E. Halpert, M.J. Panzer, M.G. Bawendi, V. Bulovic, *Nano Lett.* **9**, 2367 (2009)
12. Y. Fang, S. Chu, H. Chen, P. Kao, I. Chen, C. Hwang, *J. Electrochem. Soc.* **156**, K55 (2009)
13. T.P. Surkova, V.R. Galakhov, E.Z. Kurmaev, *Low Temp. Phys.* **35**, 79 (2009)
14. R.N. Bhargava, D. Gallagher, *Phys. Rev. Lett.* **72**, 416 (1994)
15. M.M. Rashad, D.A. Rayan, K. El-Barawy, *J. Phys. Conf. Ser.* **200**, 072077 (2010)
16. J. Yang, L. Fan, J. Cao, D. Han, M. Wei, L. Yang, B. Feng, B. Wang, H. Fu, S. Ge, *J. Mater. Sci.* **24**, 1955 (2013)
17. R. Sahraei, A. Daneshfar, A. Goudarzi, S. Abbasi, M.H. Majles Ara, F. Rahimi, *J. Mater. Sci.* **24**, 260 (2013)
18. W. Vogel, P.H. Borse, N. Deshmukh, S.K. Kulkarni, *Langmuir* **16**, 2032 (2000)
19. N. Karar, H. Chander, S.M. Shivaprasad, *Appl. Phys. Lett.* **85**, 5058 (2004)
20. D. Jiang, L. Cao, W. Liu, G. Su, H. Qu, Y. Sun, B. Dong, *Nanoscale Res. Lett.* **4**, 78 (2009)
21. A.A. Ashkarran, *Mater Sci in Semicond. Process.* **17**, 1 (2014)
22. S. Sen, C.S. Solanki, P. Sharma, *J. Lumin.* **145**, 669 (2014)
23. A. Jain, S. Panwar, T.W. Kang, H.C. Jeon, S. Kumar, R.K. Choubey, *J. Mater. Sci.* **25**, 1716 (2014)
24. H.S. Bhatti, S. Kumar, K. Singh, Kavita, R.K. Choubey, *Russ. J. Phys. Chem.* **88**, 1166 (2014)
25. D. Haranath, H. Chander, N. Bhalla, P. Sharma, K.N. Sood, *Appl. Phys. Lett.* **86**, 201904 (2005)
26. D. Haranath, N. Bhalla, H. Chander, Rashmi, M. Kar, R. Kishore, *J. Appl. Phys.* **96**, 7600 (2004)
27. B. Steitz, Y. Axmann, H. Hofmann, A. Petri-Fink, *J. Lumin.* **128**, 92 (2008)
28. R. Thielsch, T. Böhme, H. Böttcher, *Phys. Status Solidi (A)* **155**, 157 (1996)
29. M. Sharma, T. Jain, S. Singh, O.P. Pandey, *AIP Adv.* **2**, 012183 (2012)
30. N. Karar, F. Singh, B.R. Mehta, *J. Appl. Phys.* **95**, 656 (2004)
31. M.L. Steigerwald, L.E. Brus, *Acc. Chem. Res.* **23**, 183 (1990)
32. B.S. Remadevi, R. Raveendran, A.V. Vaidyan, *Pramana, J. Phys.* **68**(4), 679 (2007)
33. I. Ahemen, O. Meludu, E. Odoh, *Br. J. Appl. Sci. Technol.* **3**(4), 1228 (2013)
34. J. Alaria, P. Turek, M. Bernard, M. Bouloudenine, A. Berbadj, N. Brihi, G. Schmerber, S. Colis, A. Dinia, *J. Magn. Mater.* **286**, 297 (2005)
35. J.H. Jeong, H. Kyoung, *J. Phys. Chem.* **79**, 075413 (2009)
36. B. Stuart, *Infrared Spectroscopy: Fundamentals and Applications* (Wiley, New York, 2004)